

# A Phenomenological Model for Predicting Thermochromism of Regioregular and Nonregioregular Poly(3-alkylthiophenes)

Cheng Yang, Francesco P. Orfino, and Steven Holdcroft\*

Department of Chemistry, Simon Fraser University, Burnaby, B.C., Canada V5A 1S6

Received March 29, 1996; Revised Manuscript Received June 24, 1996<sup>®</sup>

**ABSTRACT:** Thermochromism of a series of cast films of poly(3-alkylthiophenes) (P3ATs, A = hexyl, octyl, dodecyl, and hexadecyl) with different head-to-tail (HT) diad content (70–100%) was studied. The thermochromic behavior is found to be controlled by the HT diad content and the side chain length. P3ATs with moderate HT diad content give rise to a clear thermochromic isosbestic point irrespective of the length of the alkyl side chain. Regioregular polymers possessing a >90% HT diad content exhibit either a continuous thermochromic blue shift or an isosbestic point, depending on the alkyl side chain length. The different thermochromic characteristics are attributed to subtle morphological differences between the polymers. DSC and X-ray diffraction studies indicate that P3AT samples with moderate HT regularity are formally amorphous with a quasi-ordered phase dispersed in continuous disordered domains. P3ATs with high HT regularity consist of crystalline, quasi-ordered, and disordered phases. For polymers with short alkyl side chains, these phases equilibrate with each other and destroy the thermochromic isosbestic point. Polymers with long alkyl side chains melt at much lower temperature and are converted directly between the crystalline and disordered phases.

## Introduction

An interesting and unique property of poly(3-alkylthiophenes) is their thermochromism.<sup>1–3</sup> The solid-state thermochromism of P3ATs was first reported by Inganäs' group,<sup>1a</sup> who found that the color of P3AT films changed from red-violet at room temperature to yellow at elevated temperatures. This color change is almost fully reversible in an inert atmosphere or vacuum.<sup>1</sup> Similar observations were reported by other groups.<sup>2–8</sup> The phenomenon has been attributed to the twisting of the thiophene chain with a subsequent decrease in the conjugation length.<sup>8</sup> It is generally accepted that, at low temperature, adjacent thienyl units adopt a *trans*-planar conformation which favors a longer conjugation length and a red-shifted absorption maximum. At elevated temperatures, the *trans*-planar conformation of the side chains is less stable and a *trans* to *gauche* conversion occurs with an increase in disorder of the side chains. This conversion forces the thiophene rings along the main chain to twist with respect to each other, resulting in a coiled chain with shorter conjugation lengths and a corresponding blue shift of the absorption maximum.

Detailed thermochromic analysis of P3ATs has yielded conflicting results. Inganäs<sup>1</sup> and Heeger's<sup>3</sup> groups observed a continuous blue shift upon heating the P3AT samples and proposed that the polymer possesses a multiphase morphology which changes continuously upon heating as a result of a changing chain conformation. In contrast, others claim that a clear thermochromic isosbestic point is observed, which infers that the polymer possesses a two-phase morphology.<sup>2, 8</sup> More recently, Leclerc and co-workers proposed that the existence of an isosbestic point is due to the formation of delocalized conformational defects ("twistons") which occur upon heating<sup>6</sup> as a result of conformational changes related to individual chains.<sup>7</sup>

Coupling of the 3-alkylthiophenes results in three different regiochemical diads: the "head-to-tail" diad

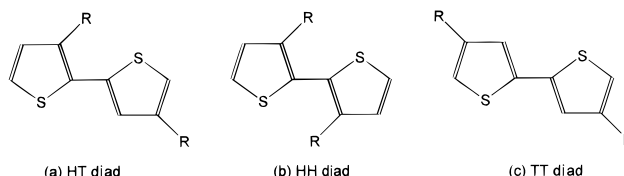


Figure 1. Diad linkages of P3ATs.

(HT), *i.e.* 2,5'-coupling, the "head-to-head" diad (HH), *i.e.* 2,2'-coupling, and "tail-to-tail" diad (TT), *i.e.* 5,5'-coupling (Figure 1). The HT diad content of P3ATs can be tuned by employing appropriate synthetic methods.<sup>9–11</sup> To date, there have been few attempts to integrate the regioregularity of P3ATs into models for thermochromism. This is surprising given that many properties of P3ATs are attenuated by changing their regioregularity. The most recent attempt to incorporate regioregularity with thermochromism was Leclerc's group,<sup>5,6</sup> who showed that the thermochromic conformational transition of P3ATs is strongly dependent on the substitution pattern; however, there does not yet exist a model which integrates all the thermochromic data reported to date.

In this work, we address the apparent contradictions that exist in the literature and report that the head-to-tail (HT) diad content and the alkyl side chain length of P3AT molecules determine the type of thermochromic behavior by affecting the morphological structure of P3AT films. It will be shown that the existence or absence of an isosbestic point can be predicted based on the structural regularity and the alkyl side chain length.

## Experimental Section

**Preparation of Poly(3-alkylthiophenes).** P3ATs (A = hexyl, octyl, dodecyl, and hexadecyl) with low to moderate HT regioregularity were prepared by oxidative coupling of the corresponding alkylthiophene using FeCl<sub>3</sub>.<sup>9</sup> <sup>1</sup>H NMR was used to determine the HT diad content of the samples, and the HT diad contents were found to be 70–84%.<sup>10</sup> In a typical experiment, poly(3-alkylthiophene) was synthesized by the following procedure. To a stirred solution of 40 mmol of FeCl<sub>3</sub> in 250 mL of CHCl<sub>3</sub> purged with nitrogen was added 10 mmol of 3-alkylthiophene. The mixture was stirred for 2 h at room

\* To whom correspondence should be addressed.

<sup>®</sup> Abstract published in *Advance ACS Abstracts*, August 15, 1996.

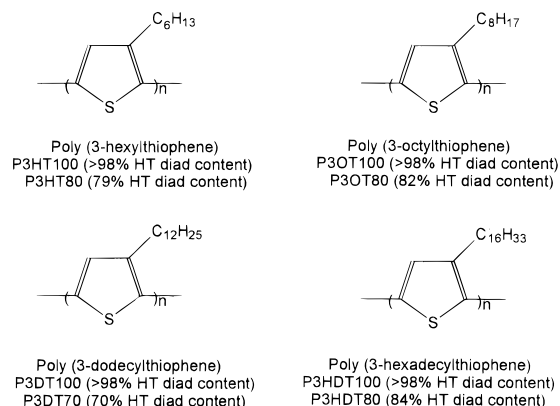


**Figure 2.** Structures and abbreviations of P3ATs used in this work.

**Table 1.** Percent HT Content, Molecular Weights, and Molecular Weight Distributions of P3ATs

sample	% HT	$M_w$	$M_n$	$M_w/M_n$
P3HT80	79	$1.70 \times 10^5$	$4.79 \times 10^4$	3.56
P3HT100	>98	$0.80 \times 10^4$	$0.65 \times 10^4$	1.22
P3OT80	82	$1.07 \times 10^5$	$3.39 \times 10^4$	3.15
P3OT100	>98	$1.61 \times 10^4$	$1.19 \times 10^4$	1.34
P3DT70	70	$1.25 \times 10^4$	$0.68 \times 10^4$	1.84
P3DT100	>98	$2.00 \times 10^4$	$1.30 \times 10^4$	1.54
P3HDT80	84	$1.12 \times 10^5$	$7.68 \times 10^4$	1.46
P3HDT100	>98	$2.25 \times 10^4$	$1.40 \times 10^4$	1.61

temperature prior to the addition of methanol whereupon a black precipitate was obtained. The precipitate was consecutively filtered, washed with methanol, 28% ammonia solution, acidic methanol and methanol. A reddish solid was obtained (50–60% yield), which was subsequently dried under reduced pressure.

P3ATs with high HT regioregularity were prepared by cross-coupling of the 5-Grignard reagent of the corresponding 2-bromo-3-alkylthiophene.<sup>11</sup> No HH diad signal could be detected by  $^1\text{H}$  NMR for P3ATs synthesized by this method. In a typical experiment, HT regioregular P3AT was synthesized by the following procedure. Into a dry round-bottom flask were placed 15 mmol of dry diisopropylamine and 75 mL of freshly distilled THF. To the mixture was added 15 mmol of *n*-butyllithium at room temperature. The mixture was then cooled to  $-40^\circ\text{C}$  and stirred for 40 min. The reaction mixture containing LDA was cooled to  $-78^\circ\text{C}$ , and 15 mmol of 2-bromo-3-alkylthiophene was added. After being stirred for 40 min at  $-40^\circ\text{C}$ , the mixture was cooled to  $-60^\circ\text{C}$  and 15 mmol of  $\text{MgBr}_2 \cdot \text{Et}_2\text{O}$  was added. After being stirred at  $-60^\circ\text{C}$  for 20 min, the reaction mixture was allowed to warm slowly to  $-5^\circ\text{C}$ , whereupon the  $\text{MgBr}_2 \cdot \text{Et}_2\text{O}$  reacted. Then 0.5 mol % of  $\text{Ni}(\text{dppp})_2\text{Cl}_2$  was added, and the mixture was allowed to warm to room temperature overnight ( $\sim 18$  h). The reaction was quenched by MeOH, and solvents were removed under reduced pressure. The red residue was subjected to Soxhlet extractions using MeOH,  $\text{H}_2\text{O}$ , MeOH, and hexane solvents consecutively, in order to remove oligomers and impurities. The polymer was then dissolved in  $\text{CHCl}_3$  using a Soxhlet extractor. Removal of solvent afforded a 30–40% yield of desired polymer.

The structure of the polymers prepared for this study, their HT diad content, and their abbreviations are given in Figure 2.

**Measurements.** Molecular weights and molecular weight distributions of P3ATs, calibrated against poly(3-hexylthiophene) standards,<sup>12</sup> were characterized by gel permeation chromatography (GPC) (Waters Model 510) using  $\mu$ -Styragel columns at  $25^\circ\text{C}$ . Polymers were eluted with tetrahydrofuran at a flow rate of 1 mL/min and detected using a UV-vis spectrophotometer (Waters Model 486) at 480 nm. The results are given in Table 1.

Thin films of P3ATs for UV-vis absorption studies were cast on glass substrates from chloroform solution at room temperature. Optical absorption spectral measurements were carried

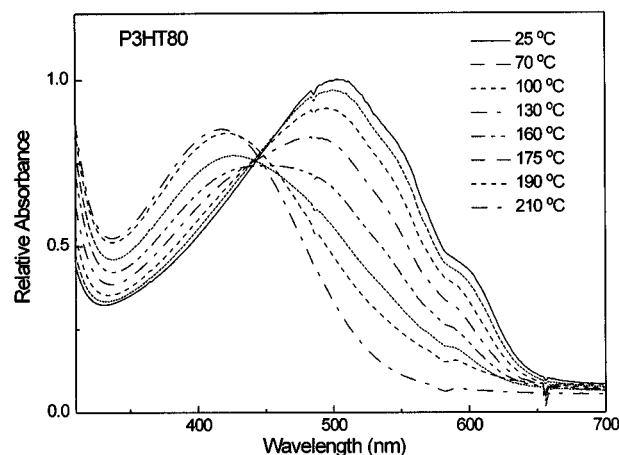


**Figure 3.** Temperature dependence of UV-vis absorption spectra of P3HT80 film.

out using a Hewlett-Packard Model HP8452A diode array spectrophotometer equipped with a custom-made temperature control cell ( $\pm 2^\circ\text{C}$ ). The temperature range investigated was between room temperature and above the P3AT's melting temperature. P3HDT100 samples were annealed prior to temperature dependence measurements. All measurements were performed under a nitrogen atmosphere.

Differential scanning calorimetry (DSC) measurements were performed on a Du Pont Model 2100 Thermal Analyst equipped with a Model 910 DSC unit. The sample, typically 8–12 mg, was pressed in a sealed aluminum pan, and the measurements were carried out using a heating rate of  $10^\circ\text{C}/\text{min}$  in ambient atmosphere. The transition temperatures were reproducible to  $\pm 2^\circ\text{C}$ , and the enthalpies of the transitions were calculated by integrating the area under the endothermic peaks. These are reported in units of kilojoules per mole of repeating unit.

Samples for X-ray diffraction studies were prepared by casting films on a copper substrate from chloroform solution at room temperature. The X-ray diffractions were obtained between room temperature and above the sample's melting point using a Siemens D5000 diffractometer with a Cu X-ray tube. The samples were mounted horizontally in a Bragg-Brentano geometry and the data were collected in  $\theta$ - $\theta$  mode from  $2$  to  $35^\circ$  in  $0.1^\circ$  intervals with a 3.6 s/point dwell time and  $1^\circ\text{C}/\text{min}$  heating rate; thus a typical scan took approximately 20 min. The peaks in each spectrum were fitted with Voigt line shapes using a fitting routine integrated with the operating system of the diffractometer.

## Results

**Temperature Dependence of UV-vis Absorption Spectra.** UV-vis absorption spectra of P3ATs with different regioregularity were recorded between room temperature and above their melting temperature. The temperature dependence of the electronic absorption spectrum of P3HT80 film is shown in Figure 3. At room temperature an absorption maximum at 502 nm was observed for P3HT80. Upon heating, the intensity of this band decreased and a new band appeared at  $\sim 420$  nm. Above  $200^\circ\text{C}$ , only the 420 nm band could be observed and, at  $\sim 450$  nm, a clear isosbestic point noted. A two-phase morphology of the sample may be inferred from the presence of an isosbestic point.

A film of P3OT80 gave rise to an absorption maximum at 510 nm at room temperature (not shown). As for the previous sample, a new band centered at 420 nm appeared with increasing temperature at the expense of the 510 nm band. At temperatures higher than  $150^\circ\text{C}$ , only the high-energy band could be observed. Again, a clear isosbestic point was observed. The thermochromic behavior of P3HT80 and P3OT80 is essentially the same, except that the transition between the two

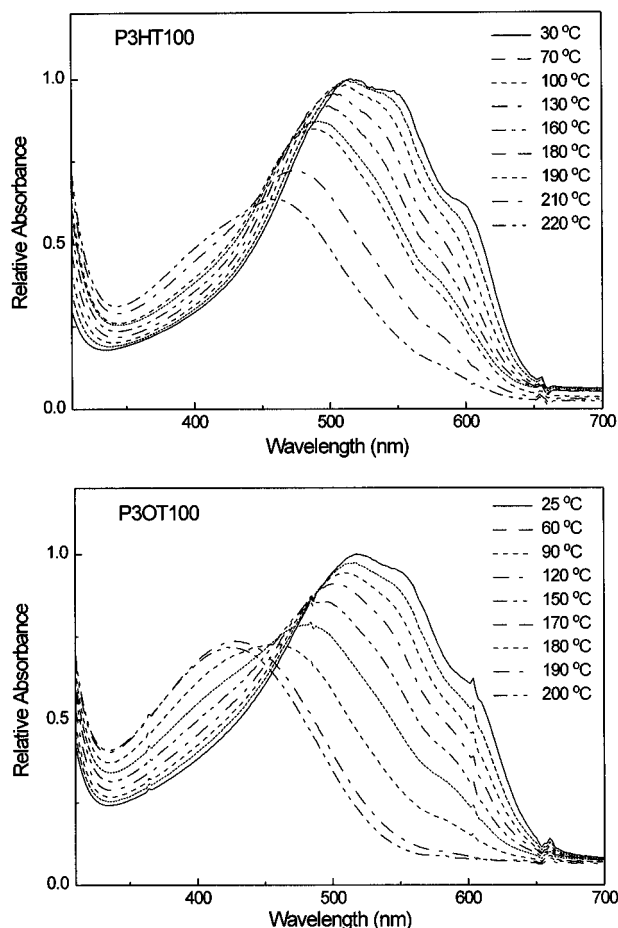


**Figure 4.** Temperature dependence of UV-vis absorption spectra of P3HT100 and P3OT100 films.

absorbing phases occurs at a lower temperature for P3OT80. Similar thermochromic behavior was observed for samples of P3DT70 and P3HDT80, although the temperature required to convert from the lower energy absorbing phase to the higher energy absorbing phase occurred at even lower temperatures (not shown).

Polymers with very high HT diad content showed a different temperature dependence of the electronic absorption spectra. Shown in Figure 4 are the absorption spectra of P3HT100 and P3OT100 films. At room temperature, P3HT100 film gave rise to an absorption maximum at 520 nm, with two shoulders at 550 and 600 nm, respectively. The 550 nm shoulder disappeared at  $\sim 160$  °C; however, the 600 nm shoulder could still be observed at 210 °C and disappeared at 220 °C. The absorption maximum at this temperature occurred at 450 nm. The absorption maximum blue shifted continuously with increasing temperature and no isosbestic point was observed. This observation infers a continuous decrease in conjugation length or a multiphase morphology of the sample.

The absorption maximum of a P3OT100 film blue shifted from 520 nm, at room temperature, to a band centered at 425 nm at 200 °C. A continuous blue shift of the absorption band upon heating could be observed up to a temperature of 170 °C. Above this temperature, a broad isosbestic point could be seen to emerge.

Shown in Figure 5 is the temperature dependence of the electronic absorption spectra of P3DT100. An absorption maximum at 526 nm, together with two shoulders at 562 and 607 nm, were observed at room temperature. The absorbance of these bands decreased,

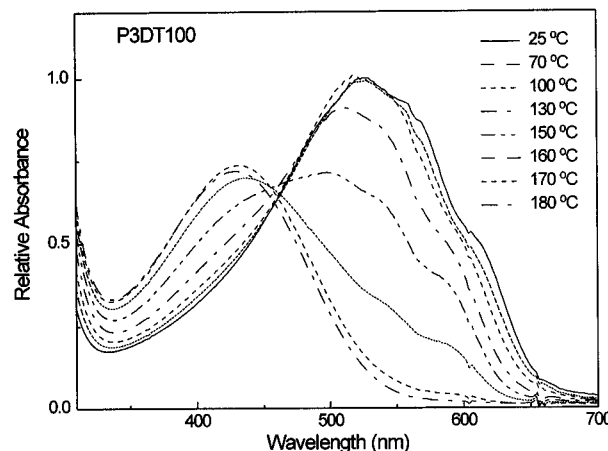


**Figure 5.** Temperature dependence of UV-vis absorption spectra of P3DT100 film.

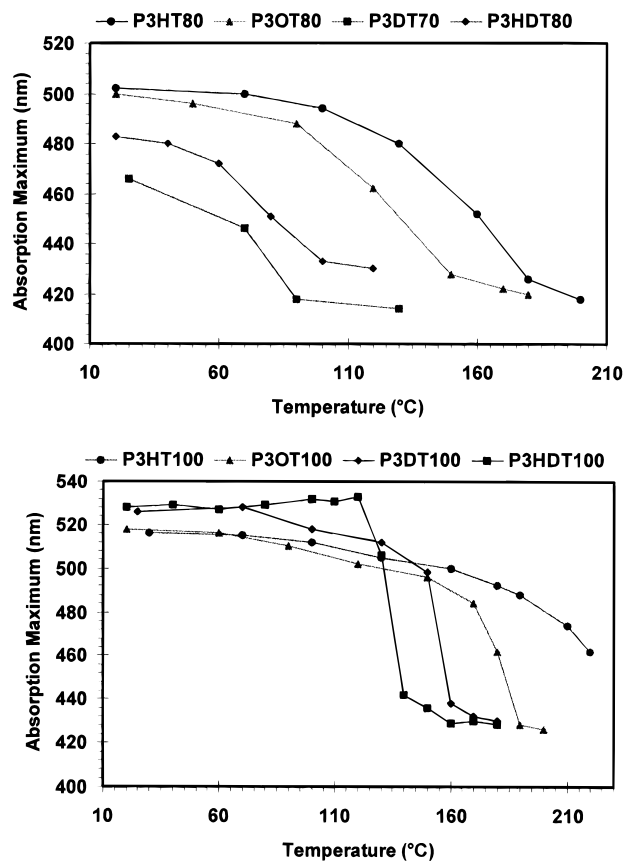


**Figure 6.** Temperature dependence of absorption maxima for P3ATs.

and a new band centered at  $\sim 430$  nm appeared and increased in intensity with increasing temperature. A broad isosbestic point was observed at  $\sim 460$  nm. Similarly, heating P3HDT100 resulted in a new band at  $\sim 430$  nm at the expense of the long-wavelength absorption band at 530 nm (not shown). A clear thermochromic isosbestic point was also observed at  $\sim 470$  nm.

A convenient way to illustrate how the regiochemistry and side chain length affect the temperature over which thermochromic transitions occur is to plot the wavelength of absorption maximum,  $\lambda_{\text{max}}$ , against the temperature (Figure 6). By inspection, all samples exhibited similar behavior, except that P3OT100, P3DT100, and P3HDT100 showed a sharp transition. The temperature at the inflection point of the curve was taken to be indicative of the temperature required to inter-

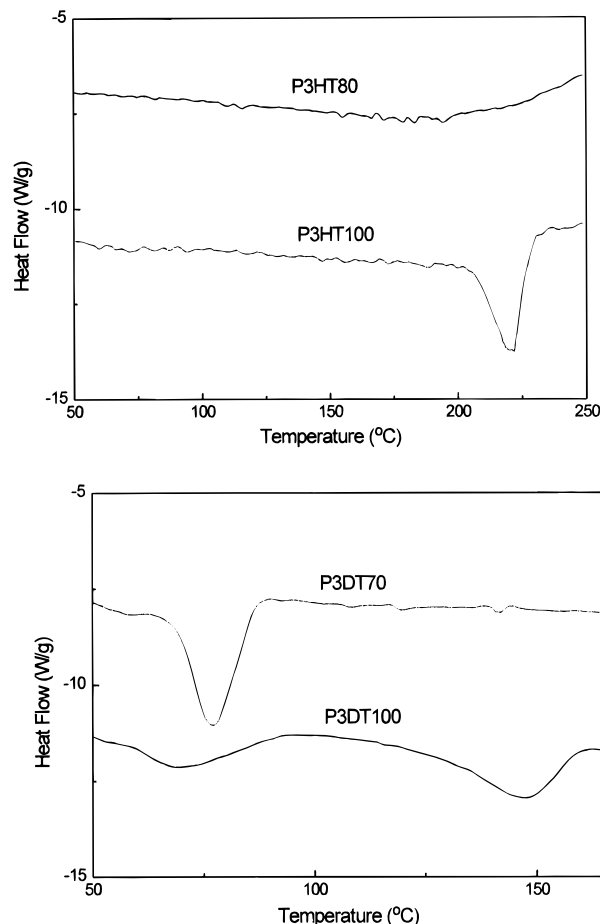


**Figure 7.** DSC thermograms of P3HT80, P3HT100, P3DT70, and P3DT100.

convert the two absorbing phases. For P3HT80, P3OT80, P3DT70, and P3HDT80, this occurred at *ca.* 180, 140, 80, and 75 °C, respectively. For regioregular samples, P3HT100 showed a continuous blue shift, while P3OT100, P3DT100, and P3HDT100, showed steep transitions at *ca.* 195, 150, and 140 °C, respectively.

**Differential Scanning Calorimetry (DSC).** The DSC thermograms of the heating scan of P3HT80, P3HT100, P3DT70, and P3DT100 are shown in Figure 7. A first-order transition was not observed for P3HT80, indicating that the sample is virtually amorphous. In contrast, an endothermic transition was observed at 220 °C with a heat flow of 3.4 kJ/mol of repeating unit for P3HT100. This first-order transition is interpreted as being due to melting of crystallites. The relatively small heat flow suggests that the sample is only semicrystalline. For P3OT80, a very small endothermic transition at 164 °C was observed with a heat flow of <0.3 kJ/mol of repeating unit (not shown). This indicates that P3OT80 film is also formally amorphous. P3OT100, however, gave rise to a first-order endothermic transition at 175 °C with a heat flow of 2.3 kJ/mol of repeating unit, indicating its semicrystalline nature.

P3DT70 gave rise to a first-order endothermic transition peak at 75 °C with a heat flow of 7.2 kJ/mol of repeating unit (Figure 7). This observation is consistent with previous DSC studies and is attributed to the disruption of ordered side chains.<sup>4,7,13,14</sup> However, the absence of a melting transition associated with crystallinity of the main chain indicates that the polymer is not crystalline. For P3DT100, first-order transitions were observed at 69 and 147 °C, respectively. The heat

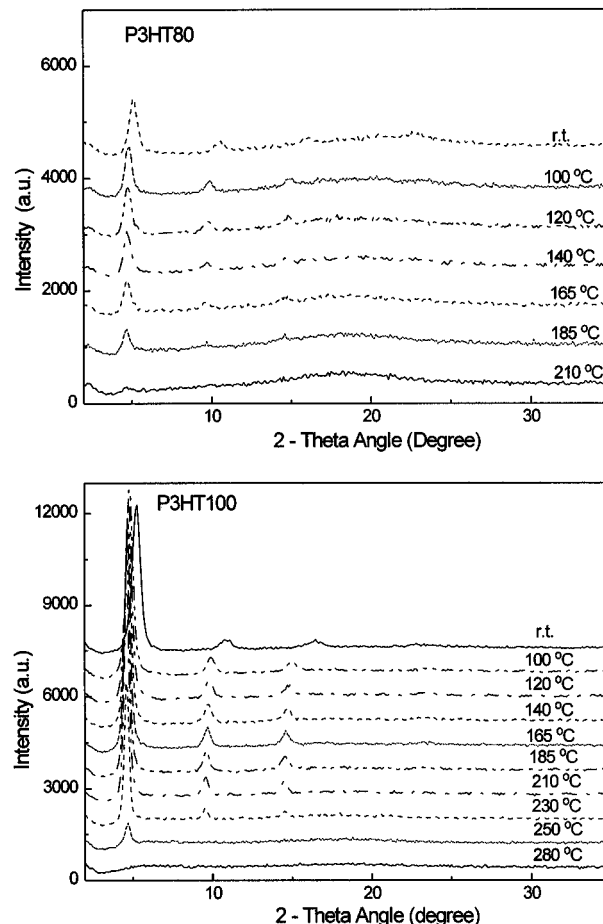


**Figure 8.** Temperature dependence of X-ray diffraction (XRD) spectra of P3HT80 and P3HT100.

flows for the two peaks were 3.8 and 3.9 kJ/mol of repeating unit, respectively. The first transition is due to the melting of ordered side chains while the second transition is attributed to the melting of main chain crystallites. The existence of separate melting transitions of ordered side chains and main chains is often observed for comblike polymers possessing alkyl side chains with ten or more carbon atoms.<sup>4,7,13</sup>

For P3HDT80, a very broad peak of the melting of side chain crystallinity with a heat flow of 5.1 kJ/mol of repeating unit was observed (not shown). Also, a small first-order transition at 126 °C with a heat flow of 1.0 kJ/mol of repeating unit was observed, which appears to be due to the melting of a small number of crystallites. For P3HDT100, a broad peak associated with the melting of side chain aggregates at 93 °C with a heat flow of 6.0 kJ/mol of repeating unit was observed. A peak associated with the melting of the main chain crystallites at 145 °C with a heat flow of 4.0 kJ/mol of repeating unit indicates that P3HDT100 is semicrystalline (not shown).

**X-ray Diffraction (XRD).** X-ray diffraction spectra for all samples were obtained. All the data sets were similar; *i.e.* regioregular samples exhibited sharper peaks than the nonregioregular counterparts. A shift to lower angles of the diffracted peak positions was observed for samples containing longer side chains. Figure 8 shows the temperature dependence of the diffraction spectra for P3HT80 and P3HT100. Diffraction peaks corresponding to the (100), (200), and (300) planes were notable for both samples.<sup>15,16</sup> In addition, P3HT80 exhibits an amorphous peak at  $2\theta \approx 21^\circ$  due

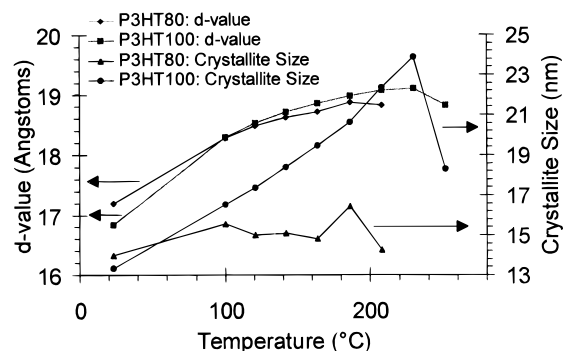


**Figure 9.** Temperature dependence of (a) the lattice spacing and (b) the crystallite size for P3HT80 and P3HT100.

**Table 2.** XRD Data for Various Poly(3-alkylthiophenes)

	(100)	exptl <i>d</i> -value (Å) <sup>b</sup>	calcd <i>d</i> -value (Å) <sup>c</sup>	crystallite size (nm)
P3HT100	5.25	16.8	17.4	13.3
P3OT100	4.20	21.0	21.7	22.9
P3DT100	3.15	28.0	30.4	120.1
P3HDT100	2.50 <sup>a</sup>	35.3 <sup>a</sup>	39.4	

<sup>a</sup> Annealed by heating to 185 °C. <sup>b</sup> *a*-axis. <sup>c</sup> Calculated according to the method given in ref 4.

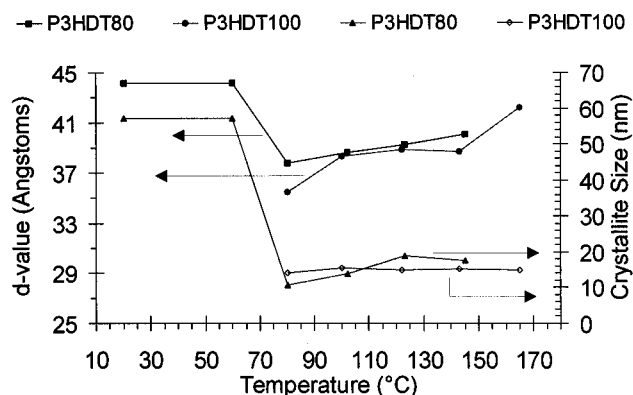
to an amorphous phase. The angular positions of the peaks were used to determine the interlayer spacing according to the standard diffraction condition.<sup>17</sup> In Figure 9 the interlamellar separations are plotted as a function of temperature for both regioregular and non-regioregular P3HT samples. A similar trend was observed, namely, an initial increase in spacing upon heating followed by a decrease at high temperature where the polymer begins to melt.

Table 2 tabulates the room temperature values of the (100) peak positions for the 100% HT regioregular polymers and their corresponding *d*-spacings. The *d*-spacing values calculated from the ideal model are also listed in Table 2. For P3HT100 and P3OT100, the calculated *d*-spacing values are very close to the experimental values. For P3DT100 and P3HDT100, however, the experimental values are substantially smaller than the calculated ones. This is consistent with a previous report where the apparent deviation of experimental *d*-spacing of P3ATs with longer side chains has been attributed to the partial intercalation of the side chains.<sup>4</sup>

The angular dispersion of the diffraction peaks (FWHM) yields information about the dimensions of the crystalline region responsible for scattering the X-rays. The crystallite size, as it pertains to the *c*-axis, and for crystallite sizes smaller than 100 nm, can be calculated using the Scherrer formula<sup>18</sup> shown in eq 1

$$t = \frac{K\lambda}{B \cos \theta} \quad (1)$$

where *t* is the crystallite size (nm), *K* is a constant (0.9),  $\lambda$  is the wavelength of the X-rays (0.15418 nm), *B* is the angular dispersion of the peak (radians), and  $\theta$  is the peak's position (degrees). We recognize that the calculated crystallite sizes are one-dimensional values and do not truly reflect the absolute sizes of crystallites. Thus we use them only to examine trends in changes in lattice dimension. The temperature dependence of the crystallite size for P3HT80 and P3HT100 is shown in Figure 9. Upon heating, the crystallite size of P3HT80, calculated from the diffracted peaks, remained constant while for P3HT100 it increased from 13 to 24



**Figure 10.** Temperature dependence of (a) the lattice spacing and (b) the crystallite size for P3HDT80 and P3HDT100.

nm. The sharp decrease in crystallite size of P3HT100 at high temperature is due to the melting of the main chain at 220 °C, as confirmed by the DSC results.

For the P3OT100 sample (not shown), a small amorphous background was noted in the XRD spectra. Fitted XRD spectra, at room temperature, also indicate the presence of a broad peak at  $2\theta = 23.9^\circ$  (*d*-value of 3.73 Å), which corresponds to the (010) reflection and may be attributed to the interlayer separation due to the  $\pi$ -stacking of the thienyl units. The crystalline diffraction peak associated with the (100) plane was shifted to a lower  $2\theta$  values compared to P3HT100 as shown in Table 2. The shift is not surprising since it indicates that the interplanar distance is larger than the hexyl analog as a consequence of the longer alkyl side chain. Upon heating, the lattice spacing for P3OT100 is consistently larger than P3HT100, as expected, due to the longer alkyl chain. The spacing increased from 21 to 23 Å upon heating from room temperature to 160 °C.

The plot of *d*-spacing, (100) plane, and the corresponding crystallite size for P3DT100 as a function of temperature (not shown) indicates that both parameters increase as a function of temperature, up to the onset of melting at 147 °C, whereupon the diffraction peaks disappeared. The *d*-spacing increases from 28 to ~31.5 Å and the crystallite size increases from 13 to 32 nm upon heating from room temperature to 140 °C. Thus, for this polymer, even though melting of the side chains was observed by DSC (Figure 7), the crystallite size still increased. This observation implies that the reordering of the main chain is not accompanied by a decrease in the crystallite size but that the crystallites' boundaries keep expanding.

Figure 10 shows the plots of the *d*-spacings and the crystallite size as a function of temperature for samples of P3HDT80 and P3HDT100. A large decrease in both of these parameters occurred for P3HT80 at ~70 °C, which coincides with the transition of the side chain melting as shown by DSC measurements. This suggests that intercalation of the side chains occurs at this temperature with a consequent decrease in the size of the crystallites and the interlamellar spacing. Upon a further increase in the temperature, the *d*-value increased from 38 to 40 Å and the crystallite size increased from 10 to 20 nm. The dramatic decrease in crystallite dimensions at 70 °C was not observed for the P3HDT100 sample, which may indicate that the side chains in this polymer are already in a substantially intercalated geometry at room temperature. This conclusion is supported by the observation that although the lattice constant for P3HDT100 is already in the same range

**Table 3. Representative Results of Thermochromic Behavior of P3ATs in the Literature**

sample	isosbestic point	HT diad content (%) <sup>c</sup>	polymerization method	ref
P3HT	yes	~80	FeCl <sub>3</sub>	4, 8
P3OT	yes	~80	FeCl <sub>3</sub>	4
P3DT	yes	~80	FeCl <sub>3</sub>	2, 4, 5b, 8, 20
P3BT <sup>a</sup>	yes	~80	FeCl <sub>3</sub>	20
P3DST <sup>b</sup>	yes	~80	FeCl <sub>3</sub>	2
P3HT	no	>90	electrochemical	3
P3HT	no	>90	Grignard coupling	1
P3BT <sup>a</sup>	no	>90	Grignard coupling	1b
P3OT	no	>90	Grignard coupling	1b
P3DT	yes	~100 <sup>d</sup>	Rieke zinc	7

<sup>a</sup> Poly(3-butylthiophene). <sup>b</sup> Poly(3-docosylthiophene). <sup>c</sup> Estimated from UV-vis spectra. <sup>d</sup> Measured by <sup>1</sup>H NMR.

as for P3HDT80, *i.e.* 36–42 Å, the crystallite regions do not expand upon further heating.

## Discussion

The nature of the thermochromic behavior of P3ATs has led to an apparent conflict in the literature. Yoshino's group<sup>2</sup> reports a clear thermochromic isosbestic point, while Inganäs' and Heeger's groups claim a continuous blue shift with increasing temperature.<sup>1,3</sup> In the late 1980s, at the time these reports were published, the scientific community paid little attention to the effect of regioregularity on the properties of P3ATs; hence, neither group reported the HT regularity of their samples. Inganäs' samples were prepared by nickel-catalyzed dehalogenating polycondensation of 3-hexyl-2,5-diiodothiophene, while Yoshino's samples were prepared by chemical oxidation of 3-alkylthiophenes with FeCl<sub>3</sub>. Gallazzi *et al.* have since shown that the former method yields P3ATs with >90% HT diad content, while the latter method yields P3ATs with ~80% HT diad content.<sup>10a</sup> A careful study of their results shows that Inganäs<sup>1</sup> used P3HT films which exhibited a room temperature absorption maximum at 516 nm (2.41 eV), indicating a >90% HT diad content. In contrast, samples used by Yoshino<sup>2</sup> exhibited an absorption maximum at ~500 nm, indicating a HT diad content of approximately 80%. Thus the controversy in the literature appears to be related to the difference in the HT regularity.

Thermochromic behavior of P3AT films as reported in the literature is shown in Table 3. In this table, we classify the HT content of samples as *ca.* 80% or >90% using reported UV-vis absorption data in cases where the HT content was not reported. The results show that P3ATs with ~80% HT diad content yield a thermochromic isosbestic point while P3AT films possessing >90% HT diad content yield a continuous blue shift. The only anomaly tabulated is P3DT with ~100% HT diad content, for which a thermochromic isosbestic point has been reported.

Our results confirm that P3AT samples of different HT diad content give rise to different thermochromic behavior. Specifically, P3HT80, P3OT80, P3DT70, P3HDT80, P3DT100, and P3HDT100 exhibit a thermochromic isosbestic point. P3HT100 yields only a continuous blue shift while P3OT100 yields a continuous blue shift up to a temperature of 170 °C and shows evidence of an isosbestic point at higher temperature. Thus, the thermochromic behavior of P3ATs is controlled by the regioregularity and the side chain length. As a consequence, some assertions may be made:

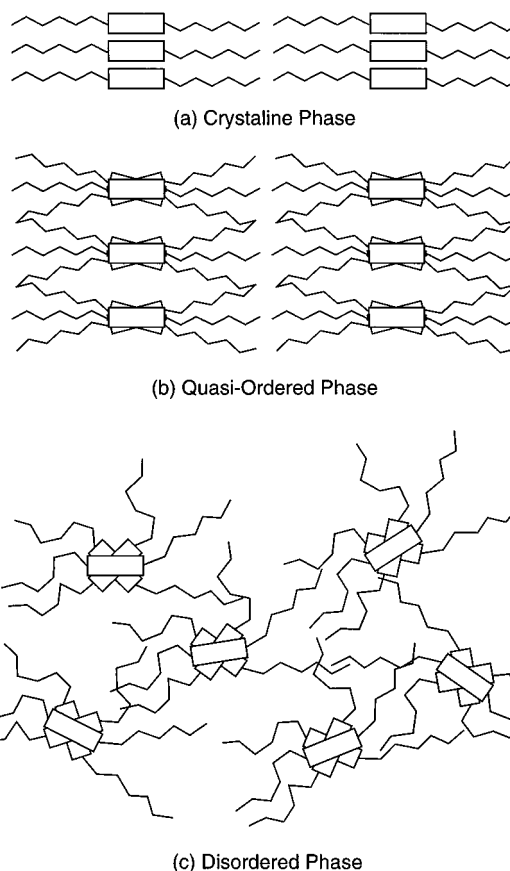


**Figure 11.** Schematic representation of (a) crystalline, (b) quasi-ordered, and (c) disordered phases of P3ATs (viewing along the thiophene chain).

samples with moderate HT content exhibit a thermochromic isosbestic point irrespective of the alkyl side chain length. HT regioregular samples with short side chains (octyl and shorter) yield a continuous blue shift of the electronic absorption band upon heating, while HT regioregular samples with longer side chains (dodecyl and longer) exhibit an isosbestic point. The discussion that follows addresses the origin of these differences.

We note that it is well known that P3ATs adopt different conformations depending on the degree of freedom of rotation about the interannular bond. In this regard, three cases can be considered: (i) in one extreme case, rotation is completely restricted and the polymer adopts a rigid-rod configuration in which adjacent thienyls are coplanar. Stacking of polymer chains in this configuration leads to highly *crystalline* regions in which the alkyl side chains adopt an *all-trans-planar* conformation<sup>1-8,19</sup> as depicted in Figure 11a. This conformation facilitates a relatively long conjugation length and hence an absorption band at longer wavelengths. (ii) In the other extreme case, interannular bond rotation can occur with little impediment, as in the case of the polymer chain in solution or in a polymer melt. In this instance, P3AT molecules assume a coiled conformation in which the thiophene rings are twisted with respect to each other, and the alkyl side chains adopt a *gauche* conformation. The twisted conformation possesses a coiled thiophene chain with relatively shorter conjugation length, and it absorbs at a relatively shorter wavelength.<sup>1-8,19</sup> In the solid state, aggregation of P3AT molecules with the twisted conformation gives rise to a *disordered* or *amorphous* phase (Figure 11c). (iii) A third state exists which lies in between the rigid

coplanar and flexible coil conformations. In this state, the interannular bond experiences some degree of freedom which allows a rocking vibration or partial twisting of adjacent thienyls, but there is insufficient freedom for adjacent thienyls to fully rotate and adopt a coiled conformation. Such a stage may occur if there are weak steric interactions due to head-to-head linkages or if the polymer possesses sufficient thermal energy. This is the *quasi-ordered* phase described by Zerbi's<sup>19</sup> and Yoshino's<sup>20</sup> groups in which the chains stack in a manner similar to the crystalline polymer but the  $\pi$ - $\pi$  interactions are weaker and the interchain distances larger. This situation is depicted in Figure 11b. In the following discussion, we propose a model which describes how the interplay and dynamic nature of these morphologies determines the thermochromic behavior of P3ATs.

It would appear reasonable to assume that heating a semicrystalline sample of poly(3-alkylthiophene) leads to an expansion of the crystal lattice due to an increase in the vibrational energy content of the polymer. In fact, for P3HT100 we observe an increase in the interlamellar spacing from 16.8 to 19.1 Å (14% increase) and an increase in the relative crystallite size from 13.3 to 18.3 nm (38% increase) as the temperature is increased from 30 to 230 °C (see Figure 9). Since the lattice expands with increasing temperature, so too will the average degree of twist along a polymer chain. As a consequence, the average degree of conjugation will decrease until the coplanarity between adjacent thienyls is totally disrupted. Essentially, this process can be viewed as converting the crystalline phase into the disordered phase via a quasi-ordered intermediate phase. Therefore, a continuously thermochromic blue-shift would be observed for this multiphase morphology, as in fact it is for P3HT100 and P3OT100.

The thermochromic behavior of P3DT100 and P3HDT100 is different, but it should be noted that both XRD and DSC analyses confirm the fact that the melting temperature of the polymer decreases as the length of the side chain is increased. For example, DSC analyses yield melting transition peaks for P3HT100, P3OT100, P3DT100, and P3HDT100 at *ca.* 220, 175, 147, and 145 °C, respectively. Thus, the temperature range over which P3HT100 is observed to exhibit a continuous blue shift is not sufficiently high to induce its melting. P3OT100 appears to undergo a continuously thermochromic blue shift in the temperature region 25–170 °C. Above this temperature, a region in which the polymer melts, an isosbestic point can be observed. In the case of P3DT100 and P3HDT100, the polymers melt at much lower temperature and the dramatic change in the absorption spectra (Figure 6) coincides with the melting temperature. Thermochromic, DSC, and XRD data indicate that upon heating, P3DT100 and P3HDT100 convert directly from the crystalline state to the polymer melt. Since these two phases have different wavelengths of maximum absorption, an isosbestic point is observed upon heating. It is also noted that above the melting temperature,  $\lambda_{\max}$  is 430 nm  $\pm$  10 nm for all polymers, which indicates a common degree of conjugation and a common conformation.

Given that P3HT100 and P3OT100 show a continuous blue shift with increasing temperature, it might be reasonable to assume that longer alkyl side chain derivatives, *e.g.* P3DT100 and P3HDT100, might also

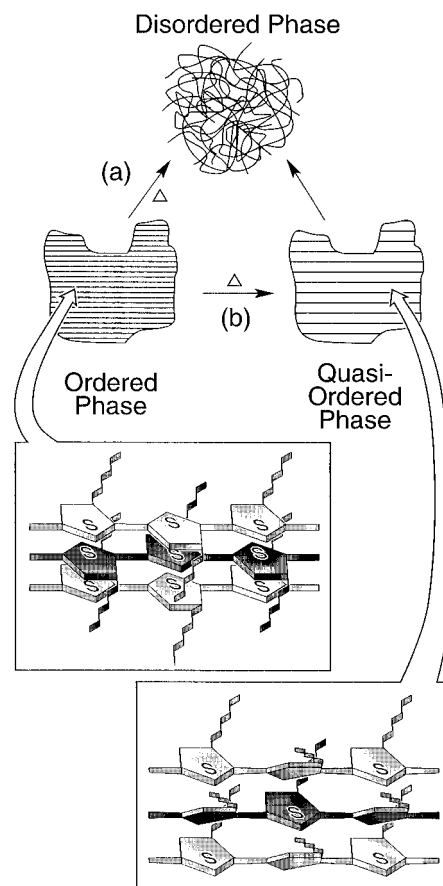


**Figure 12.** Thermomorphological transitions for regioregular P3ATs: (a) direct transition from the crystalline to the disordered phase; (b) gradual increase in the lattice spacings. Parallel lines represent  $\pi$ -stacked polymer chains.

show a continuous blue shift until they undergo melting. However, in contrast to P3HT100 and P3OT100, plots of  $\lambda_{\max}$  against temperature for P3DT100 and P3HDT100 show that  $\lambda_{\max}$  is constant until the melting temperature is reached (Figure 6). Furthermore, XRD data indicate both the crystallite size and lattice spacing of P3HDT100 remain relatively constant over this temperature range, at *ca.* 15  $\pm$  1 nm and 38.5  $\pm$  0.5 Å, respectively. As indicated by this and other X-ray diffraction results, there is significant intercalation of the alkyl side chains in the crystalline phase for P3ATs possessing long side chains.<sup>4,20</sup> This intercalation provides extra stabilization of the fully planar conformation and the crystalline structure due to the so-called "zipper effect".<sup>20</sup> Therefore, upon heating at temperatures below the melting range, only a modest blue shift of the absorption band is observed. When the melting range is reached, the entropy-favored *trans*-*gauche* transformation results in an instantaneous twisting of the skeletal chain; thus, the crystalline phase converts directly to the disordered phase and the quasi-ordered phase is bypassed. This two phase process yields an isosbestic point. Figure 12 depicts the two types of thermomorphological changes discussed above: (i) a direct transition from the crystalline to the disordered phase upon reaching the melting temperature, as observed, for P3DT100 and P3HDT100, and (ii) a gradual increase in the lattice spacings which enables a continuous disruption of  $\pi$ -conjugation (observed for P3HT100 and P3OT100). As indicated previously, P3OT100 appears to pass between the crystalline and quasi-ordered state before finally undergoing a melting transition at higher temperature.

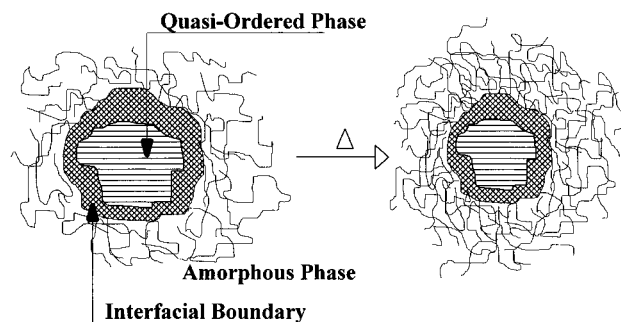


**Figure 13.** Thermomorphological transition for regioirregular P3ATs depicting the interconversion between quasi-ordered and disordered phases. Parallel lines represent  $\pi$ -stacked polymer chains.

In contrast to regioregular P3ATs, samples with lower HT content, *e.g.* P3AT80s, contain a significant proportion of sterically hindered HH couplings. Extensive crystallization of these polymers is prevented due to a twisting of adjacent thienyl units. Samples containing a moderate percentage of HT linkages, however, can still possess considerable coplanarity, which enables polymer chains to pack in a quasi-ordered state. There is some evidence of partial crystalline character in some of these regioirregular samples but the extent of crystallinity compared to the regioregular P3ATs is negligible when one compares DSC and XRD data. Thus, it is reasonable to postulate that regioirregular P3ATs are formally amorphous but contain quasi-ordered regions. The quasi-ordered and disordered phases have been reported to coexist and equilibrate with each other but at low temperatures the quasi-ordered phase dominates.<sup>8,19</sup> It has been reported that the relative concentrations of quasi-ordered and disordered phases at room temperature are 55 and 45%, respectively, for a sample with *ca.* 80% HT diad content.<sup>19</sup> The phase boundary between the quasi-ordered and disordered phases can be envisaged to be somewhat indistinct.

In our model, the percentage of disordered phase increases with increasing temperature at the expense of the quasi-ordered phase. When the temperature is sufficiently high, almost all of the quasi-ordered phase has been converted to the disordered phase. The continuous interconversion of the two absorbing phases without an intermediate during thermal cycling is responsible for the observed isosbestic point. The interconversion of the two phases is depicted in Figure 13. Indirect evidence of this thermal conversion is provided from the change of crystallite size determined by XRD. In contrast to the 38% increase in crystallite size for P3HT100 as the temperature is increased from 30 to 230 °C (see Figure 9), the crystallite size associated with P3HT80 remains constant. Since the lattice spacing of P3HT80 was found to increase by 9% over the same temperature range (see Figure 9), the number of chains per crystallite must be decreasing with increasing temperature.

## Conclusions

The thermochromic properties of P3ATs are controlled by the head-to-tail diad content and the alkyl side chain length of the sample. Samples with moderate HT diad content gave rise to a clear isosbestic point, while samples with high HT diad content and short alkyl side chains exhibit no isosbestic point with increasing temperature. This is due to a morphological effect. P3ATs

with moderate HT diad content are formally amorphous with some short-range ordered structure dispersed in the disorder bulk. The coexistence and interconversion of the two phases are believed to be responsible for the observed isosbestic point. P3ATs with high HT diad content and short alkyl side chains are semicrystalline. The crystalline, quasi-ordered, and disordered phases equilibrate with each other in the thin film. The isosbestic point is destroyed by this multiphase equilibrium. P3ATs with high HT diad content and long alkyl side chains are also semicrystalline. These samples melt at much lower temperature, converting crystalline phase directly into disordered phases; therefore, a broad isosbestic point is observed.

**Acknowledgment.** This research was sponsored by the Natural Sciences and Engineering Research Council of Canada. C.Y. thanks the Simon Fraser University (SFU) for graduate fellowships. We thank Dr. M. Abdou for designing the temperature-control cell and Mr. J. Lowe and Dr. M. Lebedev for assistance in synthesizing polymer samples. We also thank Prof. Jeff. Dahn of the Department of Physics, SFU, for the utilization of XRD and DSC apparatus.

## References and Notes

- (1) (a) Inganäs, O.; Salaneck, W. R.; Österholm, J.-E.; Laakso, J. *Synth. Met.* **1988**, *22*, 395. (b) Inganäs, O.; Gustafsson, G.; Salaneck, W. R. *Synth. Met.* **1989**, *28*, C377. (c) Salaneck, W. R.; Inganäs, O.; Nilsson, J.-O.; Österholm, J.-E.; Thémans, B.; Brédas, J.-L. *Synth. Met.* **1989**, *28*, C451.
- (2) (a) Yoshino, K.; Park, D. H.; Onoda, M.; Sugimoto, R. *Solid State Commun.* **1988**, *67*, 1119. (b) Yoshino, K.; Park, D. H.; Onoda, M.; Sugimoto, R. *Jpn. J. Appl. Phys.* **1988**, *27*, L1612. (c) Tashiro, K.; Ono, K.; Minagawa, Y.; Kobayashi, M.; Kawai, T.; Yoshino, K. *J. Polym. Sci., Polym. Phys. Ed.* **1991**, *29*, 1223.
- (3) Winokur, M. J.; Spiecel, D.; Kim, Y.; Hotta, S.; Heeger, A. J. *Synth. Met.* **1989**, *28*, C419.
- (4) Chen, S.-A.; Ni, J.-M. *Macromolecules* **1992**, *25*, 6081.
- (5) (a) Roux, C.; Leclerc, M. *Macromolecules* **1992**, *25*, 2141. (b) Roux, C.; Bergeron, J.-Y.; Leclerc, M. *Makromol. Chem.* **1993**, *194*, 869. (c) Leclerc, M.; Roux, C.; Bergeron, J.-Y. *Synth. Met.* **1993**, *55–57*, 287. (d) Roux, C.; Faid, K.; Leclerc, M. *Makromol. Chem., Rapid Commun.* **1993**, *14*, 461. (e) Roux, C.; Bergeron, J.-Y.; Leclerc, M. *Makromol. Chem.* **1993**, *194*, 869.
- (6) Roux, C.; Leclerc, M. *Chem. Mater.* **1994**, *6*, 620.
- (7) Faid, K.; Frechette, M.; Ranger, M.; Mazerolle, L.; Levesque, I.; Leclerc, M.; Chen, T.-A.; Rieke, R. D. *Chem. Mater.* **1995**, *7*, 1390.
- (8) Iwasaki, K.; Fujimoto, H.; Matsuzaki, S. *Synth. Met.* **1994**, *63*, 101.
- (9) Sugimoto, R.; Takeda, S.; Gu, H. B. *Chem. Express* **1986**, *1*, 635.
- (10) (a) Gallazzi, M. C.; Castellani, L.; Zerbi, G.; Sozzani, P. *Synth. Met.* **1991**, *41–43*, 495. (b) Sato, M.; Shimmizu, T.; Yamauchi, A. *Synth. Met.* **1991**, *41–43*, 551.
- (11) McCullough, R. D.; Low, R. D.; Jayaraman, M.; Anderson, D. L. *J. Org. Chem.* **1993**, *58*, 904.
- (12) Holdcroft, S. J. *Polym. Sci., Polym. Phys. Ed.* **1991**, *29*, 1585.
- (13) Hsu, W.-P.; Levon, K.; Ho, K.-S.; Myerson, A. S.; Kwei, T. K. *Macromolecules* **1993**, *26*, 1318.
- (14) Bolognesi, A.; Porzio, W.; Provasoli, F.; Ezquerro, T. *Makromol. Chem.* **1993**, *194*, 817.
- (15) Mårdalen, J.; Samuelsen, E. J.; Gautun, O. R.; Carlsen, P. H. *Synth. Met.* **1992**, *48*, 363.
- (16) Luzny, W.; Pron, A. *Synth. Met.* **1995**, *69*, 337.
- (17) Cullity, B. C. *Elements of X-Ray Diffraction*, 2nd ed.; Addison-Wesley: Reading, MA, 1978.
- (18) Bodor, G. *Structural Investigation of Polymers*; Ellis Horwood Ltd.: Chichester, West Sussex, England, 1991.
- (19) Zerbi, G.; Castellani, L.; Chierichetti, C.; Gallazzi, C. *Chem. Phys. Lett.* **1990**, *172*, 143.
- (20) Tashiro, K.; Minagawa, Y.; Kobayashi, M.; Morita, S.; Kawai, T.; Yoshino, K. *Synth. Met.* **1993**, *55–57*, 321.